Efficacy of Use of A-Si EPID as Imaging Device in IMRT QA

Dina Abdelaziz, Wafaa Khalifa and Nader El Sherbini

Abstract: *When IMRT treatment is considered to be a routine work, one should seek for an accurate, time saving, fast and simple QA procedure. Electronic portal imaging device (EPID), especially amorphous silicon type, is a promising tool for IMRT dosimetry. In this work a calibration of an amorphous silicon flat panel-type imager (Elekta iViewGT, release 3.2) is done, which was incorrect (figure 3.1.) due to the EPID renormalization to the target value (Elekta instructions). The calibration of the amorphous silicon flat panel-type imager (Elekta iViewGT) was repeated after considering the Pixel Scaling Factor (PSF), which gave the correct response (figure 3.2.). By using Omni Pro software the EPID images are converted into doses and a correction for the dose reading from these images is done to obtain the same results as that measured at the isocenter in 20 cm PMMA slab phantom. A correction for the EPID profiles for different field sizes is done to be like those measured in the full scatter water phantom. A pre-treatment verification for a clinical step & shoot IMRT plan is done for a prostate cancer case generated by Xio (version 4.2.2) treatment planning system (TPS). The pre-treatment verification is done by EPID and a comparison in dose distribution against TPS and Films are performed. This study show that the combination between iViewGT and Omni Pro software with the corrections provided in the present study gave an accurate method to verify the dose of IMRT fields in two dimensions inside a homogenous slab phantom. The results indicated also that the EPID (Elekta iViewGT) is an accurate and can replace film for field-by field pretreatment verification of IMRT inside a phantom.*

I. Introduction

The challenge of external beam radiotherapy for cancer treatment is to irradiate the tumor with a desired dose, while the surrounding healthy tissue suffers as little as possible radiation damage.

Due to increase of complexity in modern radiotherapy techniques the needs for checking accuracy of the delivered dose to patient has been also increased, either pretreatment or in vivo. This reflects the importance of quality assurance (QA) as a step in radiation therapy treatment.

Quality assurance procedures of a patient treatment can be divided into two main parts:

Quality control of the technical aspects of the linear accelerator (Linac) itself includes verification of: Dose output, the transferred parameter between treatment planning system (TPS) to linac (collimator settings, the direction of wedges and multileaf collimator (MLC) shape) and Isodose check.

Verification of the actual patient treatment, including verification of both patient setup and delivery of correct dose.

Ionization chamber is the predominant tool used to check the dose accuracy at certain points, while the dose distribution of certain plan could be measured using different tools, e. g. Films, 2D diode array. The increasing of using IMRT to deliver conformal radiation treatment has prompted the search for a faster and more cost effective quality assurance (QA) system. The standard technique relies on the use of film for two-dimensional dose distribution verification. Although film is considered the standard and most widely used for this purpose, the procedures involved are relatively lengthy, labor intensive and costly for multiple field IMRT verification. (Lim S. 2008).

QA of intensity modulated radiation therapy (IMRT) is a sophisticated and time consuming task, where one should check not only the delivered dose and dose distribution but also need to check the field segments shape, number and machine capability to deliver IMRT plan. When IMRT treatment is considered to be a routine work, one should seek for an accurate, time saving, fast and simple QA procedure. Electronic portal imaging device (EPID), especially amorphous silicon type, is a promising tool for IMRT dosimetry. A commercial a-Si EPID has been studied by Talamonti C., et al, (2006) to investigate its potential in the field of pretreatment verifications of step and shoot, IMRT for 6 MV photon beams.

An a-Si EPID has been investigated by Budgell G., et al, (2005) to determine its usefulness and efficiency for performing linear accelerator quality control checks specific to step and shoot IMRT. Several dosimetric parameters were measured using the EPID: dose linearity and segment to segment reproducibility of low dose segments, and delivery accuracy of fractions of monitor units. Xu C., et al, (2002) have developed an automated image based method for MLC positioning verification using images acquired from an EPID. Yeo I. (2007) developed a method based on dose-response function, which verifies the beamlet intensity in IMRT from dose image in EPID and reconstructs dose in a patient. Greer P., et al, (2007) determined the difference in response between an a-Si EPID to the open and MLC transmitted beam components of IMRT beams. Ansbacher

W. (2006) developed a method for rapid evaluation of IMRT plans, using portal images for reconstruction of the dose delivered to a virtual 3D phantom.

II. Materials And Methods

Elekta Precise (Crawley, UK) linear accelerator, which support IMRT deliver, was used in this study (figure 2.1a). This linear accelerator (LINAC) produces photon energies of 6 and 15MV, also it produces electrons with energies of 6, 8, 10, 12 and 15 Mev. Only 6 MV photon beam is used in this study. The LINAC is equipped with MLC. The MLC consists of 40 leaf pairs with 1 cm leaf width at the isocenter.The type of EPID used throughout this study is an amorphous silicon flat panel-type imager (Elekta iViewGT, release 3.2).The detector panel is a PerkinElmer Amorphous Silicon (a-Si) detector, and provides a resolution of 1024×1024 16-bit pixel images, with a detector panel size of 41×41 cm^2 (approximately 26×26 cm^2 at isocenter).Display pixel factor information;When images are acquired by iViewGT^{TM}, the pixel values are re-normalized or averaged before the image data is saved to the database. At the time of acquisition, the pixel scaling factor is saved with the images in the database. This feature allows us to determine the original accumulated pixel value by dividing the **pixel value** by the **pixel scaling factor.**Polymethyl methacrylate (PMMA), also known as acrylic. Trade names are Lucite, Plexiglas or Perspex. It consists of 1 cm for each sheet of density 1.19 g/cm3 and area 30 x 30 cm^2.GAFCHROMIC® EBT2 Dosimetry Film (8x10 in size) was used. The film spatial resolution >5,000 dpi (dots per inch) with dose range 1cGy – 10Gy (in red color channel).Omni Pro^{TM} IMRT is software used for complete dosimetric verification and QA of IMRT treatment cycle. This software function is to import and compare calculated doses fromTPS planned data with measured dose distributions from films that were exposed in the IMRT phantom. It includes 1D profile, 2D isodose profiles as well as fully automated comparisons using analysis tools such as Gamma index method.A computerized welhÖfer WP 700 water phantom version 3.5 was used in the present study for acquiring the beam data.XiO treatment planning system (TPS) (from CMS Inc., USA) version 4.2.2 implemented superposition algorithm is used in this study.

Calibration of the EPID Several steps are necessary to reconstruct the dose in the phantom or patient from the pixel values of the EPID. All measurements of this study were performed at gantry and collimator angle 0°.

A- Calibration of EPID response to different doses:EPID images of reference field size (typically 10x10 cm^2) were recorded for different MU (2, 5, 10, 15, 25, 50, 100, 150 and 200 MU).The acquired images by iViewGT^{TM} are re-normalized (automatically by the iViewGT^{TM}) before saving process; which means that all images will appear with the same optical density (OD) for all different doses images. Sofor each image the **pixel scaling factor (PSF)** is recorded to determine the original accumulated pixel value by dividing the **pixel value** by this factor

$$\text{Original accumulated pixel value} = \frac{\text{Pixel value}}{\text{Pixel Scaling Factor} \quad (PSF)} \qquad (1)$$

To convert these images into doses, all images were exported to Omni Pro system.The Omni Pro software can read the Optical Density OD of the image.Each EPID image imported to Omni Pro will be corrected for its own PSF.even after dividing each image by its corresponding PSF it will still incorrect because of several reasons:The scattered radiation from EPID;The scatter within the phantom;The scatter from the phantom to the EPID;The attenuation of the beam by the phantom; andThe distance from the radiation source to the EPID plane and to the dose reconstruction plane. (**Wendling M., et al, 2006**).Record the Omni Pro reading value for each EPID dose, and get the Dose correction factor (DF), which is the Omni Pro reading value for a specific dose divided by the Actual irradiated dose at isocenter

$$DF = \frac{\text{Omni Pro reading value for a specific dose}}{\text{Actual irradiated dose}} \qquad (2)$$

B- Calibration of the EPID profile

In order to determine the necessary parameters for correcting the dose profile reconstruction, i.e., relating pixel values in the EPID images with absolute dose values in the phantom, the EPID images at different square field sizes are recorded with PMMA slab phantom of thickness 20 cm(an average thickness to encompass the phantom (or patients) thickness at 6 MV photon beam). For all phantom measurements an isocentric setup [SAD (source –axis distance) setup] was used. Dose profiles for the same field sizeswere obtained using semiflex 0.147 ion chamber in the full-scatter water phantom [Source-Skin Distance (SSD) = 88.6cm] were measured with ion chamber at 11.4cm depth.Where 11.4 cm water is equivalent to 10 cm of Perspex. These dose profiles will be the reference for EPID dose profile correction. The EPID images were taken and corrected by PSF & DF.   After the conversion of EPID pixel values into dose values according to the dose response relation, the resulting image is called dose image D^{EPID}. The corrected portal pixel dose according to its position

regarding to central axis (CAX) is PD$^{\text{EPID}}$, which is the image after profile correction, is obtained by the predicted equation based on the previous work by **Wendling, et al, 2006 and Renner, et al, 2005**.

$$PD_{ij}^{\text{EPID}} = D_{ij}^{\text{EPID}} \times e^{-ar} \quad (3)$$

Where r is the distance of a pixel ij from the central axis, a is the exponential fitting constant.This constant is fitted properly for all field sizes.

Pre-treatment verification: EPID versus filmA clinical step & shoot IMRT plan is used for a prostate cancer treatment generated by Xio (version 4.2.2) TPS. This plan consists of seven fields, and each field had between 8-14 segments.With EPID, one image was acquired for each segment using single exposure option in the image acquisition mode for IMRT (Pre- segment image acquisition and storage also allows verification of MLC leaf position), where the dose construction was also done separately for each segment. All of these images were sent to the Omni Pro and corrected according to the previous corrections.The film irradiated simultaneously with the corresponding EPID image acquisition for each field using PMMA phantom. A film is placed at 10 cm depth in the PMMA phantom on the Linac table and 10 cm of PMMA slabs are placed under the film to achieve the backscatter. This simultaneous irradiationto avoid any fluctuation in doses between film and EPID irradiation like dose, dose rate fluctuation and MLC reposition. These images are compared with the simultaneously irradiated films and a γ evaluation was done in two dimensions.

III. Results &Discussion

3.1 EPID Response

Wendling, et al, (2006) stated that the resulting response of the a-Si EPID has been shown to be linear with dose, although a small ghosting effect remains, which is mainly a function of the number of exposed frames and no correction for ghosting effect was made in their study. So, in the present study the original accumulated pixel values of the raw images data which are obtained from iViewGT$^{\text{TM}}$ software, by using equation (2-1) as described in section (2) were used.
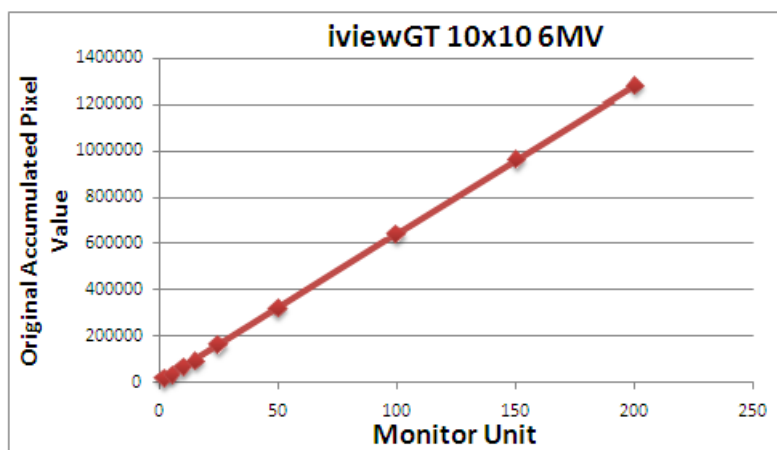
Figure (3.1.) central axis original accumulated pixel values versus monitor units for a 10x10 cm^{2}field.

3.2 Pixel Scaling Factor

Table (3-1) shows the signal reading in Omni Pro software of the doses calculated at the isocenter at 10cm depth in a 20cm thick PMMA slab phantom at SSD = 90cm.

Table (3-1)the signal reading in Omni Pro software of the doses calculated at the isocenter at 10cm depth in a 20cm thick PMMA slab phantom at SSD = 90cm.

Dose mGy at the isocenter of the PMMA phantom	Signal reading 100%
20	479
50	513
100	520
150	521.5
200	521.5
250	521.7
500	521.6
1000	521.6
2000	521.6

These signals readings were obtained without any correction where one can found that there is incorrect response,so all of these images numerical values will be divided by the PSF values listed in table (3-2). These PSF are obtained from EPID row image data.

Table (3-2) The PSF for different doses at the isocenter at 10cm depth in a 20cm thick PMMA slab phantom at SSD = 90cm for reference field size 10x10 cm^2

Dose (mGy)	PSF
20	4.61207
50	1.98999
100	0.93866
150	0.67392
200	0.51005
250	0.41549
500	0.20685
1000	0.10175
2000	0.05091

The resulting signal reading (100%) that irradiated to different doses 2,5,10, 50,100 and 200 cGy at the isocenter at 10cm depth in a 20cm thick PMMA slab phantom at SSD = 90cm for reference field size 10x10 cm^{2}after dividing all images values by the corresponding PSF using the equation (2-1), that are obtained by Omni Pro show different response for the different doses, as indicated in table (3-3).

Table (3-3)the signal reading in Omni Pro software after dividing each image numerical values by its own PSF using equation (2-1).

Dose mGy at the isocenter of the PMMA phantom	Signal reading 100%
20	103.4
50	257.5
100	554
150	773
200	1021
250	1254
500	2519
1000	5120
2000	10230

3.3 Dose Correction Factor

Although the Omni Pro gave a linear relationship between the dose and the signal reading for the EPID images after dividing by PSF, the Omni Pro signal reading is not the same as the incident dose values. These results agree with those obtained by **Wendling,et al, (2006).**

Wendling,et al, (2006) attributes these incorrect results to that the scatter within the EPID, the scatter within the phantom, the scatter from the phantom to the EPID and the attenuation of the beam by the phantom are not considered. Also the distance from the radiation source to the EPID plane and to the dose reconstruction plane is not considered.

From our results the discrepancies may also be attributed to the introduction of a proposed sensitometric curve which is the relation that consolidates Omni Pro to read the EPID images.
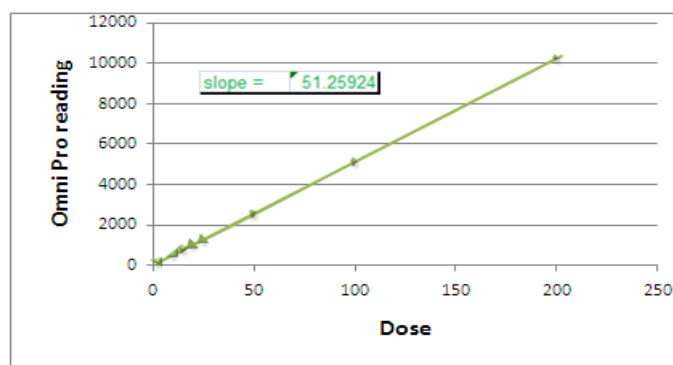
Figure (3.2.) The relation between Omni Pro reading and doses.

It is clear from figure (3.2.) that the relation between Omni Pro reading and the delivered doses is a linear relationship, and its slope = 51.26. By using equation (2-2) then the Omni Pro signal reading is the dose at the isocenter at 10cm depth in a 20cm thick PMMA slab phantom at SSD = 90cm.

Table (3-4) Dose correction factor (DF) factor for different doses that obtained using equation (2-2).

Dose mGy at the isocenter of the Perspex phantom	DF
20	51.70
50	51.50
100	55.00
150	51.53
200	51.05
250	50.16
500	50.38
1000	51.20
2000	51.15
Average value of DF	51.51

It is obvious from table (3-4) that the average DF factor is nearly the same as the slope of linear relationship of figure (3.2.), this slope = 51.26.

So the slope value of the linear relationship between the dose and the signal reading for the EPID images is used as DF value for different doses.

In this case the signal reading in Omni Pro is the same as that irradiated at the isocenter at 10cm depth in a 20cm thick PMMA slab phantom at SSD = 90cm.

Figure (3.3.) shows the two dimensional dose distributions for the EPID images after PSF and DF correction.

(a) 2CGy　　　　　　　　**(b) 5CGy**

(c) 10CGy　　　　　　　**(d) 50CGy**

(e)100CGy   **(f) 200CGy**
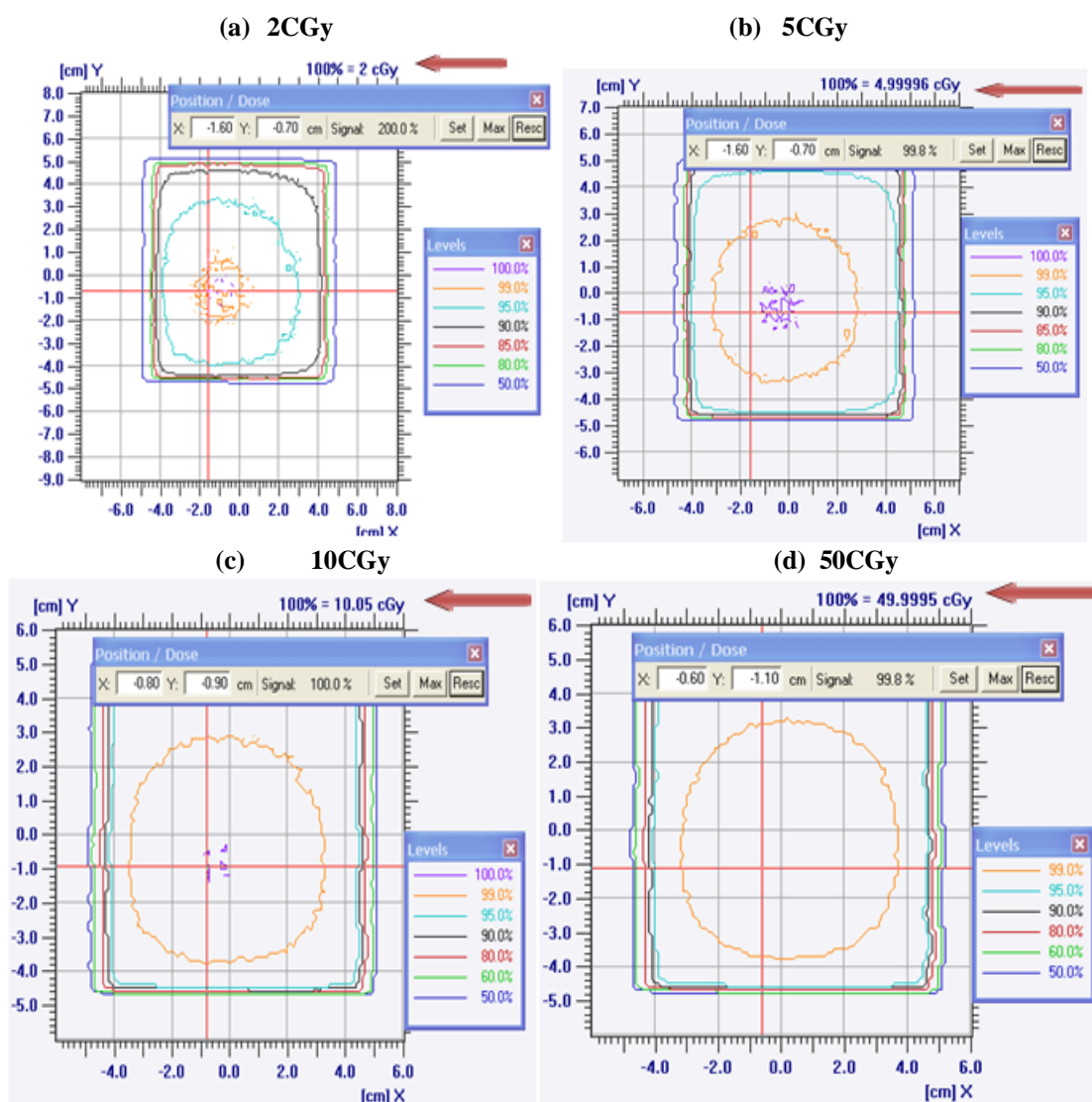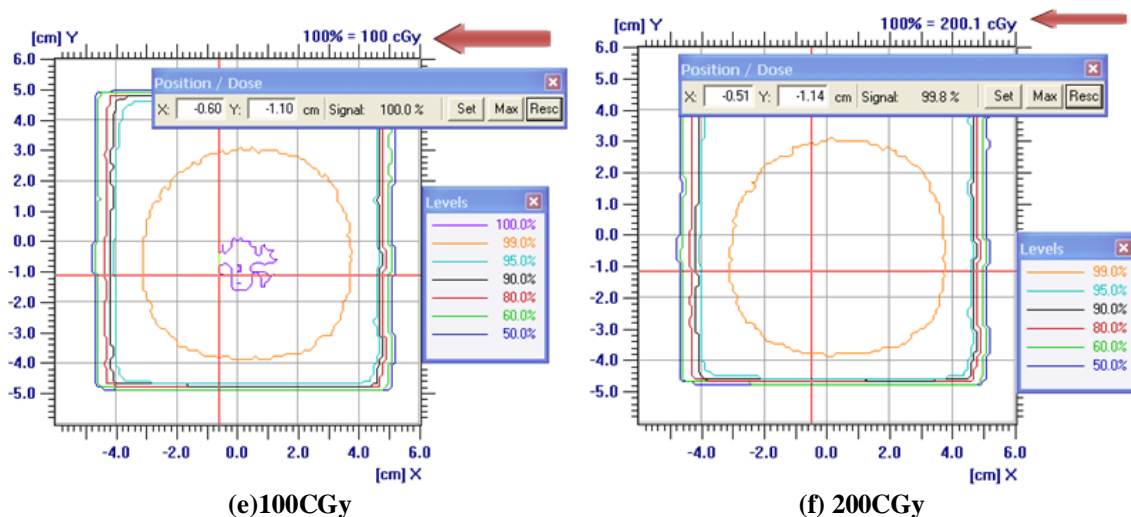
Figure (3.3.) Two dimensional dose distributions for the EPID images for 10x10 cm^2 of 6MV photon beam after PSF & DF correction

3.4 Dose correction for different field size

Table (3-5) shows the PSF for different field sizes with the same delivered doses (500 mGy).
Although all the field sizes were irradiated to the same dose at the isocenter at 10cm depth in a 20cm thick PMMA slab phantom and at SSD = 90cm, there was difference in the PSF values, which is due to the different contribution of scatter by changing the field size.

Table (3-5): PSF for different field sizes using 500 MGY.

Field size	PSF
3×3	0.1688
5×5	0.20515
10×10	0.20683
15×15	0.20022

These differences in PSF values for the different field sizes receiving the same dose at the isocenter at 10cm depth in a 20cm thick PMMA slab phantom and at SSD = 90cm may be due to the dose calculation for each field size is in full scatter conditions, that takes into consideration the collimator scatter factor and the phantom scatter factor (calculated under full scatter situation), on the other hand EPID is not a full scatter phantom **(Varian Portal Vision instructions).**

Also the EPID is known to have a lateral scatter **(Wendling,et al, 2005)** which is not considered in the full scatter phantom calculation.
By trial it was found that the PSF for the reference field 10x10 cm^2 gave approximately the same dose value for different field sizes, as tabulated in table (3-6).

Table (3-6): OmniPro maximum signal reading for different field size images obtained by EPID after dividing by the PSF of the reference field (10×10 cm^2).

Field size	Signal reading 100%
3×3	2563
5×5	2562.9
10×10	2562.9
15×15	2562.9

Then after dividing the signal reading for each image of the different field sizes by the DF (51.26) the correct dose at the isocenter, at 10cm depth in a 20cm thick PMMA slab phantom and SSD = 90cm is obtained with maximum difference ± 0.2 % as shown by the red arrow in figure (3.4.).

(a) 3×3 cm²   **(b) 5×5 cm²**
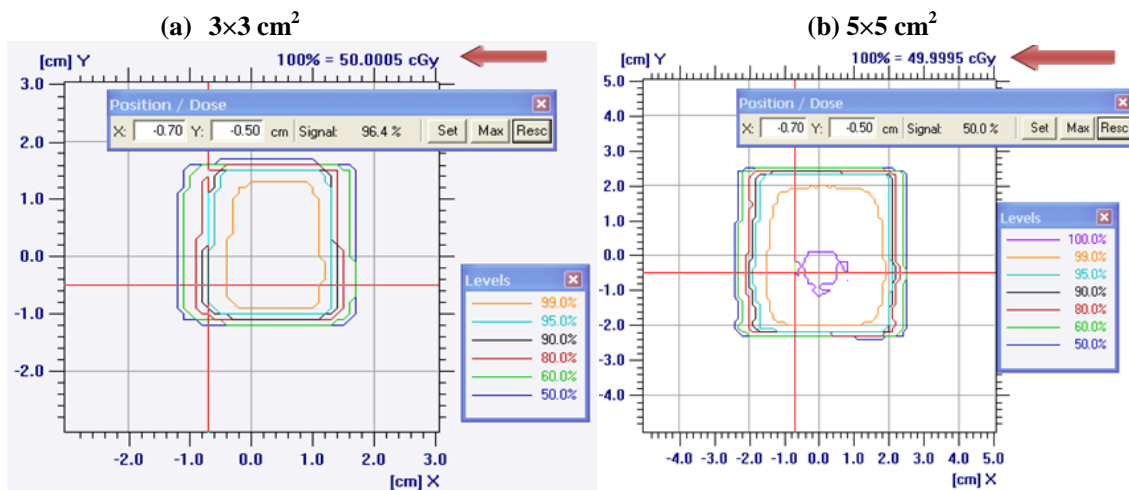
Figure (3.4.)

Generally after DF correction either for different doses of the reference field size 10×10cm² or for the same dose at different field size the average dose values agreed with the ionization chamber measurements at the isocenter at 10cm depth in a 20cm thick PMMA slab phantom at SSD = 90cm with ± 0.2 % (which agree with work done by **Wendling,et al, 2006 and Renner,et al, 2005**).

3.2 Profile Correction:

Profiles of square fields from EPID images were compared with those measured using an ionization chamber that was located in a full-scatter water phantom. Figure (3.5.) shows the actual dose profiles of square fields of different sizes obtained by EPID against the water phantom and TPS. The measurements are performed in water phantom at 11.4 cm water (which is equivalent to 10 cm of PMMA), and source skin distance (SSD) = 88.6 cm.

(a) Field size 3×3 cm²
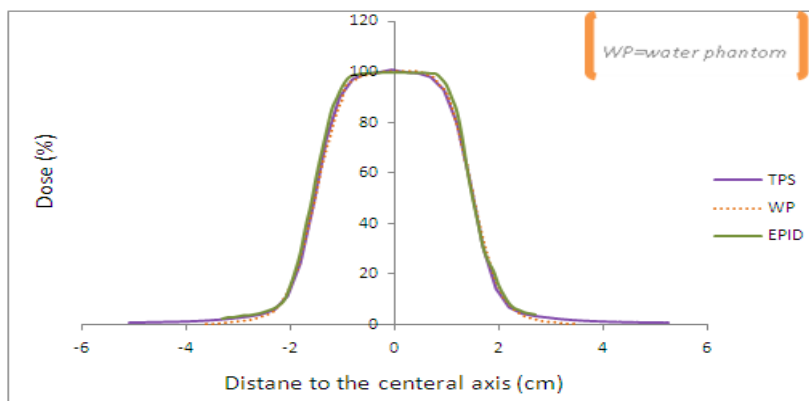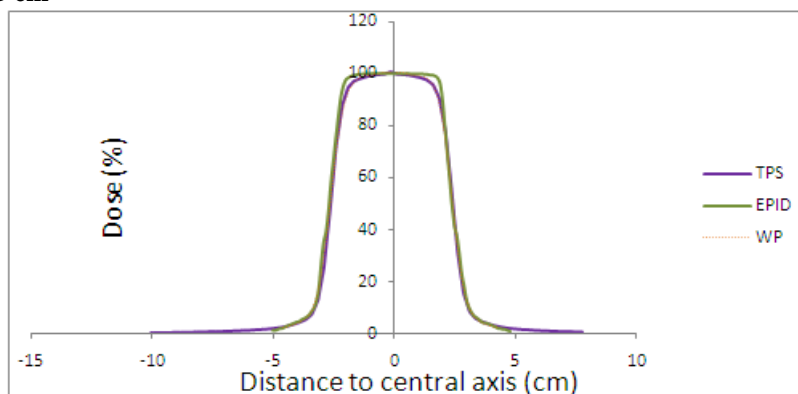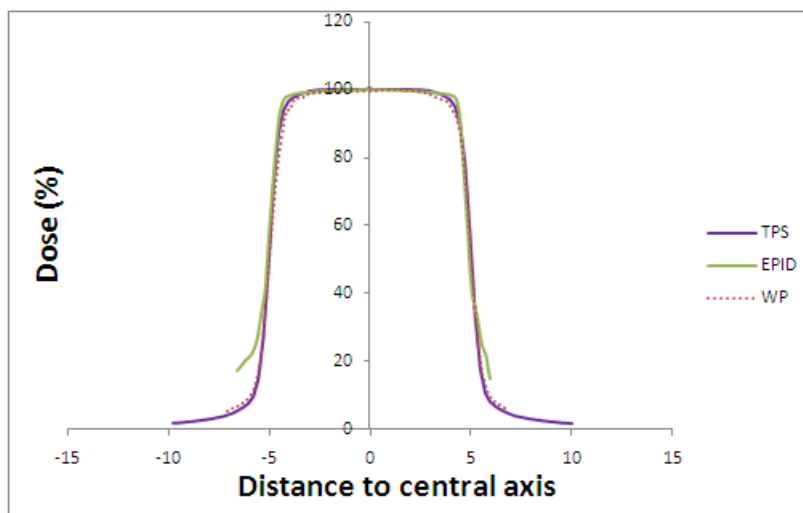
(b) Field size 5×5 cm²

(c) Field size 10×10 cm²

Figure (3.5.) dose profile as measured by water phantom and from TPS against the reconstructed dose profile from the EPID images without profile correction (a) 3×3 cm2 field size. (b) 5×5 cm2field size. (c) 10×10 cm2 field size. All profiles are normalized to 100% of the measured dose.

Figure (3.5.) shows a difference between water phantom measurements and the reconstructed profiles from the EPID images for the studied field sizes.

Table (3-7) show the maximum percent of error between profiles measured and t he EPID at different field sizes.
Table (3-7) (% error) between EPID and the water phantom dose profiles.

Field size(cm²)	Error (%)
3×3	3%
5×5	3.5%
10×10	3%

It is clear from figure (3.5.) and table (3-7); that the profile behaviour along the central axis region by the three methods is good, and became worse in the penumbra region and the tails. This is because within the EPID mainly lateral X-ray scatters and optical photon scatter occurs, resulting in more flattened at the shoulders more than in water phantom &TPS. These findings are in agreement with the results of **Wendling, et al, 2006**. The fit parameter [a] in equation (2-3) correct for these behaviour where it is obtained from the water phantom measurements.
Figure (3.6.) shows the dose profiles of square fields for different sizes obtained by EPID after correction using equation (2-3) and water phantom and TPS.

(a) Field size 3×3 cm²
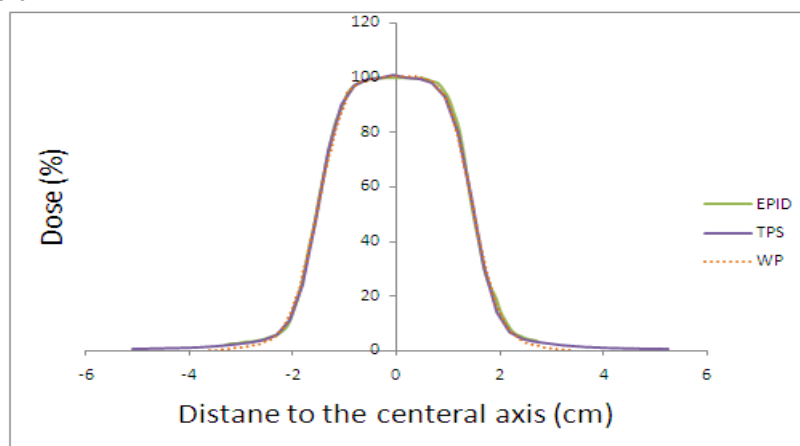
(b) Field size 5×5 cm^2
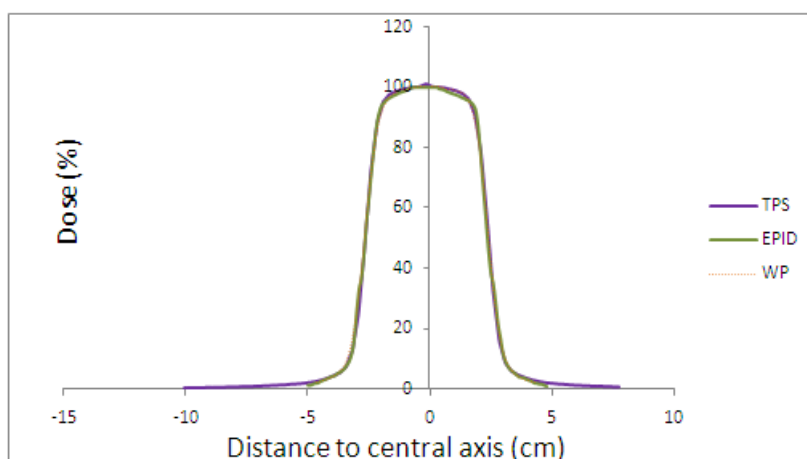
(c) Field size 10×10 cm^2
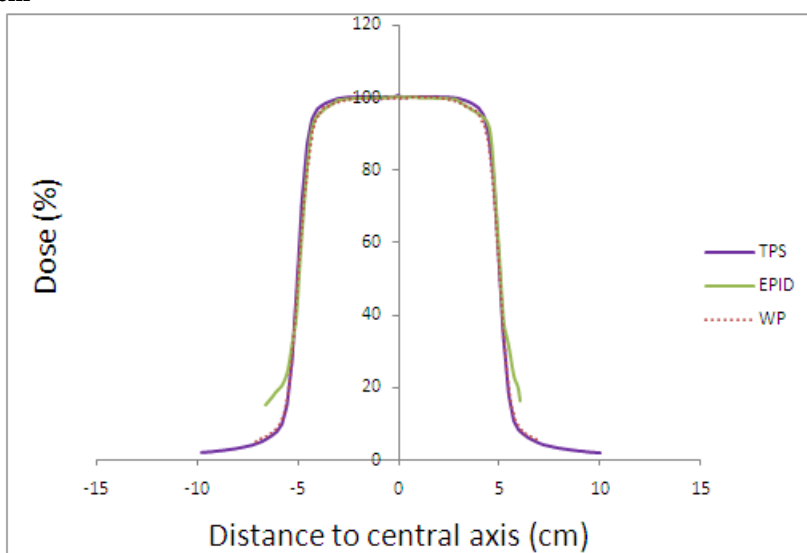
Figure (3.6.) dose profiles for different square field sizes as measured by water phantom at the isocenter at 11.4 cm depth which is equivalent to 10 cm Perspex, TPS and profiles reconstructed by the EPID using the Omni Pro software at 6MV photon beam.

The fitting constant (a) in equation (2-3) was got by iteration to minimize the variation between the measured dose by the water phantom and the reconstructed dose from the EPID, and it was found to be 0.03 for all field sizes studied.

Figure (3.6.) shows that the agreement has improved and become in agreement with the other methods (water phantom and TPS).

Among all field sizes the error does not exceed 0.2% between the EPID profiles and the profiles measured by the water phantom and calculated by the TPS except for field size 10×10 cm^2 where the agreement is down to the 30 % dose on the central axis. These findings were found to be in qualitative agreement with **Wendling M., et al, 2006** who stated that the agreement was very good with the central axis, but remain worse in the penumbra and in the tail of the profiles due to blurring of the measurements by the ionization chamber) but in this study the most importance is for the small field sizes in order that the small segments in the IMRT verification and the entire profiles for small field sizes agree with the measured ones.

Figure (3.7.) shows the difference between the EPID after dose and profile correction against the TPS for different field size with the gamma evaluation (with criteria 3mm and 3%) using the Omni Pro software and after implementing the dose and profile correction factor.

The plane dose profile comparison between the corrected EPID images and TPS is taken arbitrary on the periphery of the field, to be sure that it correct through out the field.

(a)   (b)

(c)
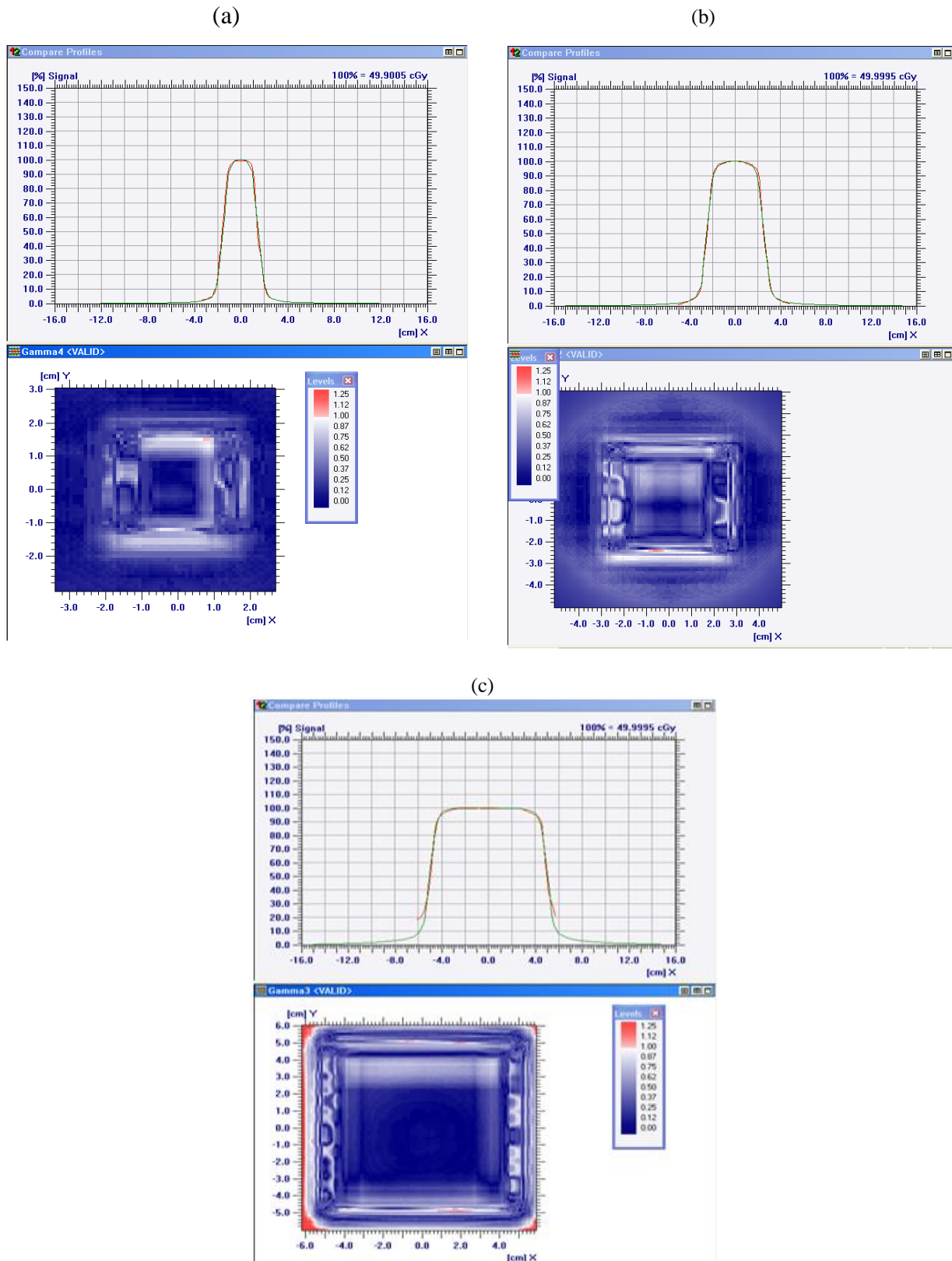
Figure (3.7) Workspace – Omni Pro IMRT QA program reveal the dose profile of the EPID against that of TPS (upper) and the γ index (upper) figure (a) for 3×3 field size, (b) for 5×5 field size and (c) for 10×10 field size. Be sure that there is no red area (γ index > 1) within the field.

3.3 Pre-treatment IMRT Verification
 a) Segment by segment:
Now, instead of using ordinary open fields, an IMRT plan distribution is displayed by EPID & films in comparison with the TPS.

The plan is done using superposition algorithm. For an IMRT case, 7 fields were used. The number of segments in each field is illustrated in the plan report, (table 3-8).

Plan Report:
Table (3-8): number of segments for a prostate IMRT plan using Xio TPS version (4.2.2).

An IMRT plan has 7 fields	
Beam number	Number of segments
1	14
2	9
3	9
4	12
5	13
6	8
7	8

The correction factors (PSF, DF & profile correction equation) will be applied to each segment for every field.

EPID in comparison with Films versus TPS
Figures from (3.8.) to (3.10.) show some of the seventh field segments as an examples with their dose distribution comparisons in terms of dose profile and theγ evaluation for EPID,as compared with film versus TPS. The γ evaluation issued to judge about the comparison on the basis of the standard deviations in the γ index between EPID & films using the Omni Pro software after all correction factors.

Since the dose for each segment was within 5-10 MUs which are under the response of Gafchromic films, the doses were normalized to 50 cGy within the isocenter.
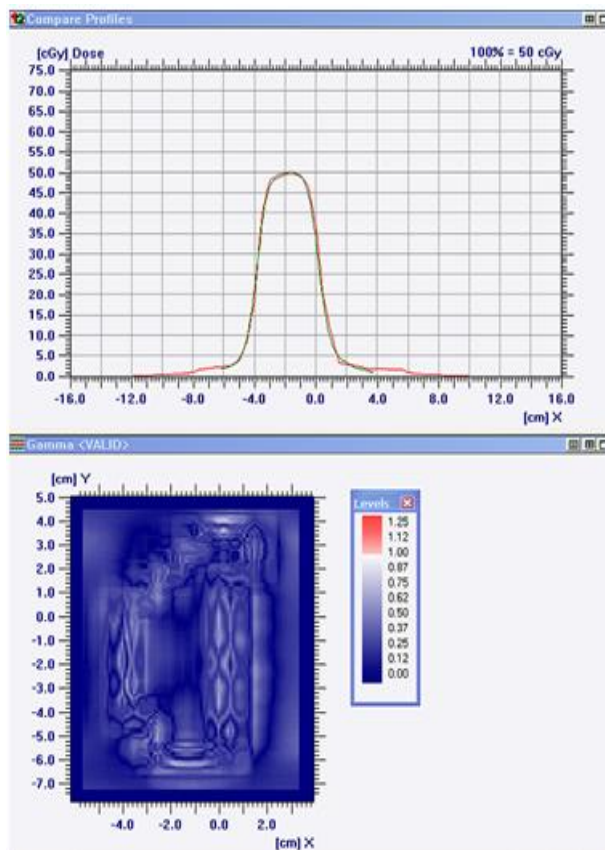
Figure (3.8, a)   Workspace – Omni Pro IMRT QA program for segment 2 reveal the dose profile of the EPID against that of TPS (upper) and the γ index (down).
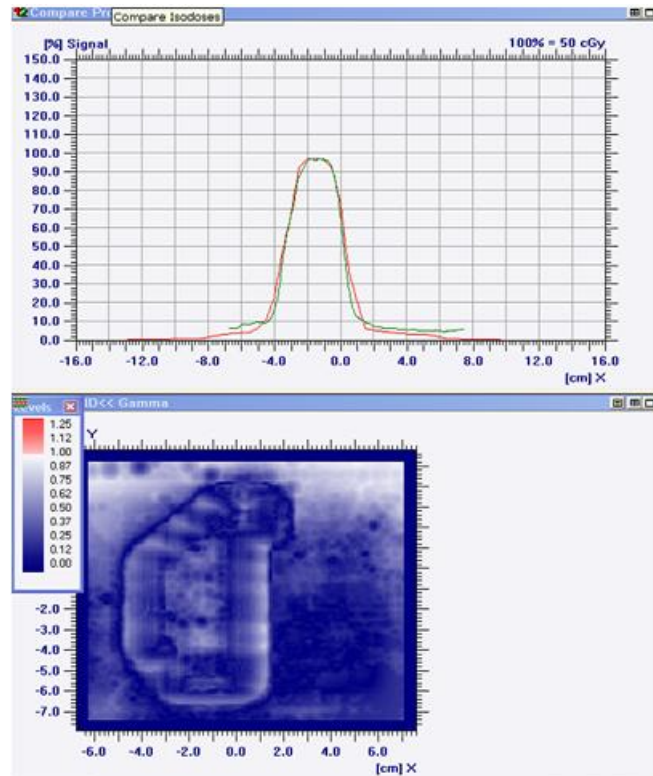
Figure (3.8, b) Workspace – Omni Pro IMRT QA program for segment 2 reveal the dose profile of the film against that of TPS (upper) and the γ index (down).
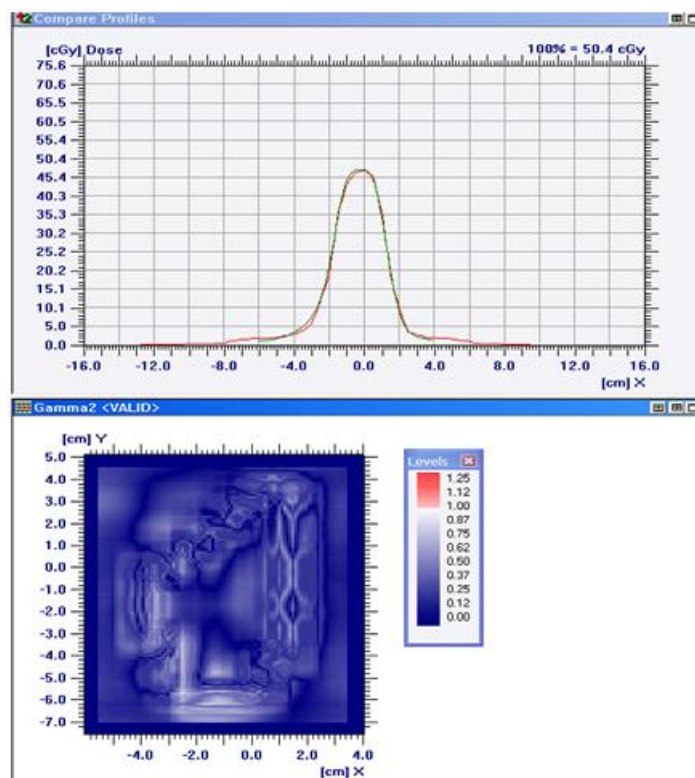
Figure (3.9, a)   Workspace – Omni Pro IMRT QA program for segment 3 reveal the dose profile of the EPID against that of TPS (upper) and the γ index (down).
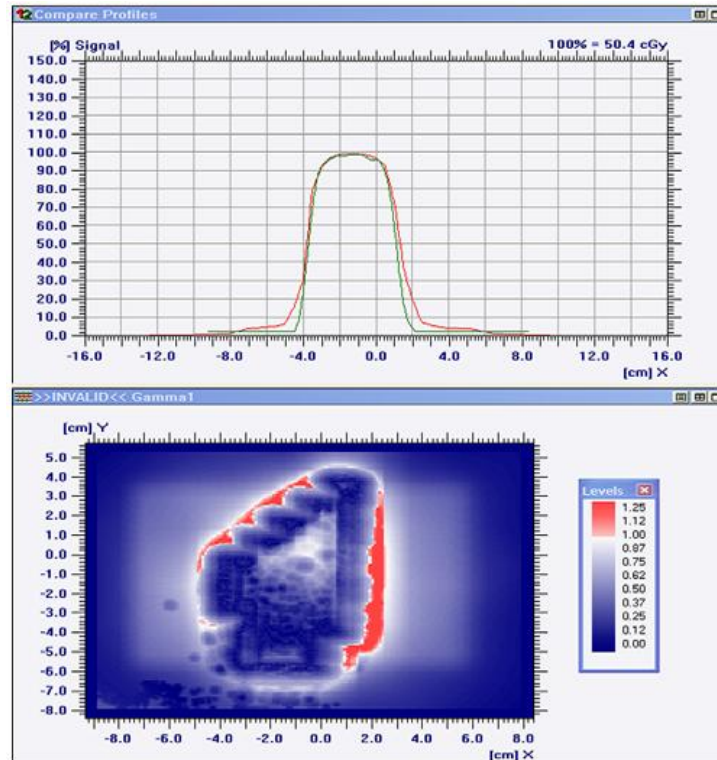
Figure (3.9,b) Workspace – Omni Pro IMRT QA program for segment 3 reveal the dose profile of the film against that of TPS (upper) and the γ index (down).
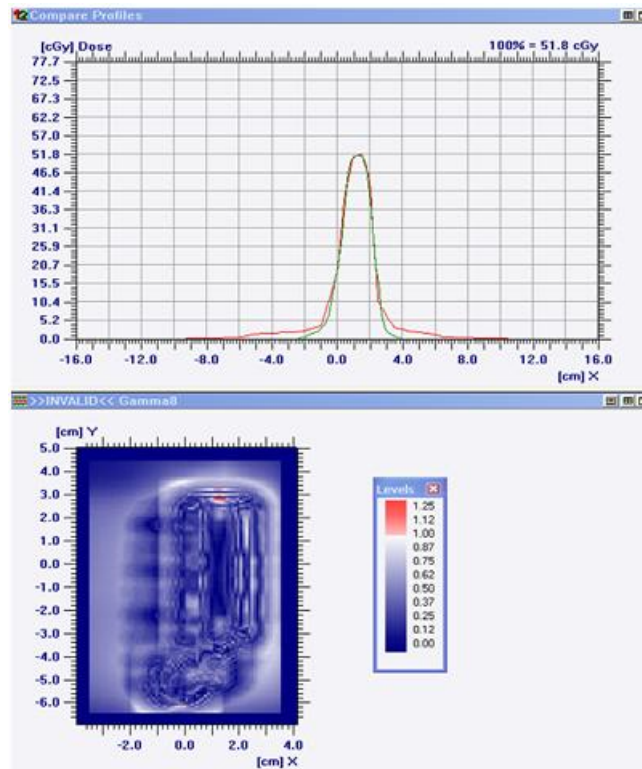
Figure (3.10, a) Workspace – Omni Pro IMRT QA program for segment 7 reveal the dose profile of the EPID against that of TPS (upper) and the γ index (down).
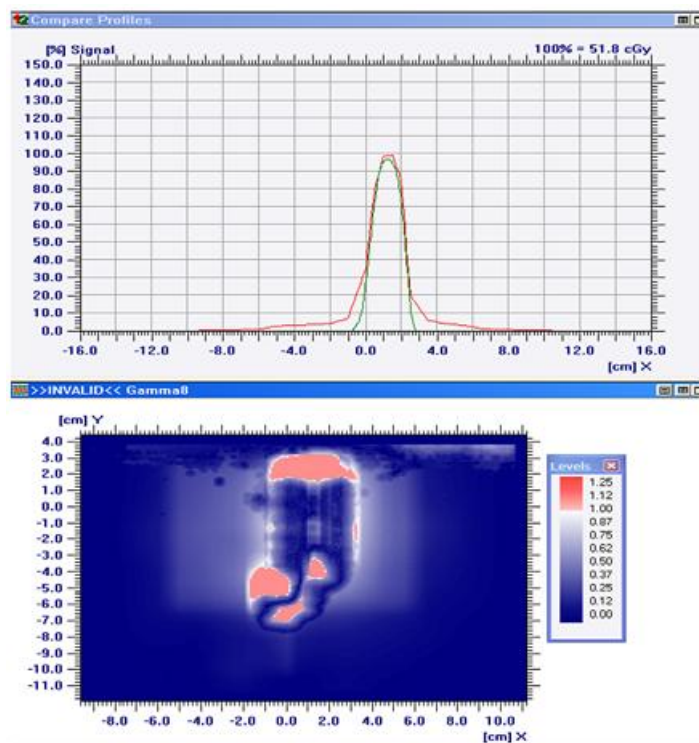
Figure (3.10,b) Workspace – Omni Pro IMRT QA program for segment 7 reveal the dose profile of the film against that of TPS (upper) and the γ index (down).

Table (3-11) show the gamma evaluation for segments as comparison between EPID & films of the present study.
Table (3-11): the standard deviation (SD) for both EPID and films in comparison to TPS using Omni Pro software for the segments of field number 7

Segment number	EPID SD %	Film SD %
1	0.24	0.31
2	0.14	0.23
3	0.15	0.29
4	0.19	0.30
5	0.23	0.28
6	0.36	0.38
7	0.23	0.24
8	0.27	0.29
Average	0.22	0.29

As seen from table (3-11); the values of the SD and the average among the 8 segments for EPID are less than that for Gafchromic films. This may be due to that the scanning of the film is not reproducible as the EPID, and even by using the protocol in the method of film scanning (taken from **Estro booklet 9 (2008)**) there is still a deviation, where scanning is done for the film more than 5 times which is an evidence on the instability and turning the scanner off between scanning this may be contributed to the total error because the condition will not be the same for all films, especially that the results will be affected if the orientation of the film is inversed. Also **Alber M., et al, (2008)** stated that if there is any defect in the film manufacturing it will strongly affect the results.

If the values of standard deviation for EPID and films in table (3-11) are analyzed separately, it will be clear that as the shaping of the segment increase with the MLC the SD relatively increases. **Renner,et al, 2005** stated that the superposition algorithm is generally known to be more accurate at tissue interfaces but it does not model either multileaf collimator leaf-end leakage or inter-leaf leakage. So increasing the number of segments in a plan will demonstrate any inaccuracy of the planning system.

On the other hand the difference between Films and EPID can also be compared by the percentage of pixels passing the gamma test in the region of interest for each segment of the field as demonstrated by the histogram in figure (3.19.).
Khan F., et al, (2008) also used the percentage of pixels passing the digital gamma test to compare between EPID and the Matrixx (in this study films used instead of MatriXX, IMRT MatriXX is a two dimensional ion chamber array (IBA Dosimetry, Schwarzenburck,Germany))
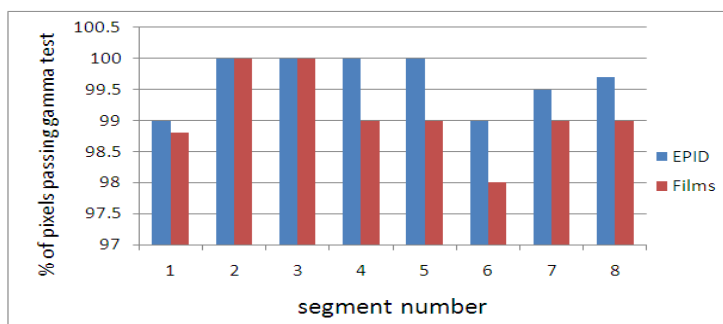
Figure (3.11.) shows the percent of pixel passing the gamma test for EPID against films.

From figure (3.11.) it is clear that for all segments the percent of pixels passing the gamma test for EPID is better than that for films. Also the minimum number of pixels passing the gamma test for EPID and film were 99% and 98% respectively for segment 8. For segments 2 and 3, all pixels pass the gamma test for both EPID and films.

Figures (3.8.) to (3.10.) show the comparison between EPID and films for samples of the segments in the seventh field. These results prove that the EPID can replace films in IMRT QA.

b) Segment combination: Finally, it important to show the difference between reconstructed dose distribution from EPID after correction and the calculated dose by TPS in the fields as a total with the same prescribed doses for the planed prostate case plan. The two-dimensional midplan (isocentric-plan) dose distributions for all segments of each field were then summed to obtain the total midplan dose of that specific field. Figure (3.12, a) show Workspace – Omni Pro IMRT QA program for the a field from IMRT plan for the prostate case with its prescribed doses that calculated by the TPS in the PMMA slab phantom(at 10 cm depth and SSD=90) at gantry zero. The difference in dose distribution between the calculated dose by TPS and the reconstructed dose distribution by EPID is also presented in the figures. Figure (3.12, b) show the histograms of the γ index, indicating the maximum, minimum signal, the average signal and the standard deviation for each field using EPID.
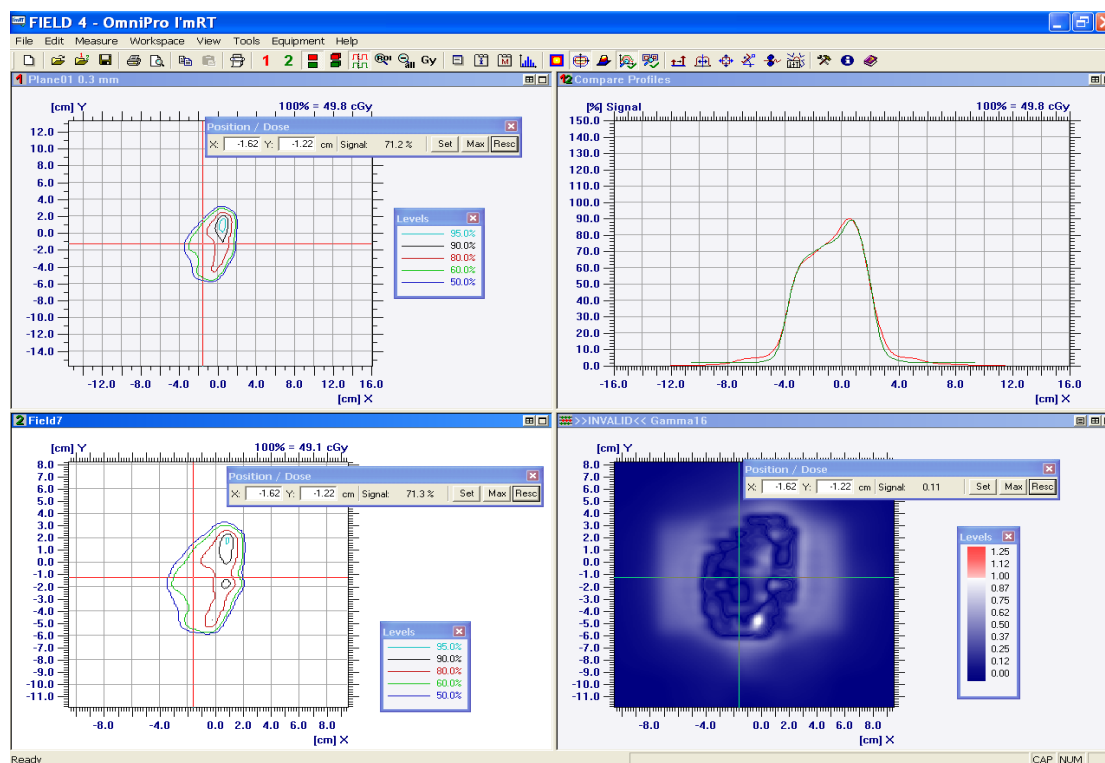
Figure (3.12, a) Workspace – Omni Pro IMRT QA program for field 7, reveal the dose distribution of the EPID(down-left),the TPS dose distribution (upper-left),the dose profile of the EPID against that of TPS (upper-right) and the γ index (down-right).
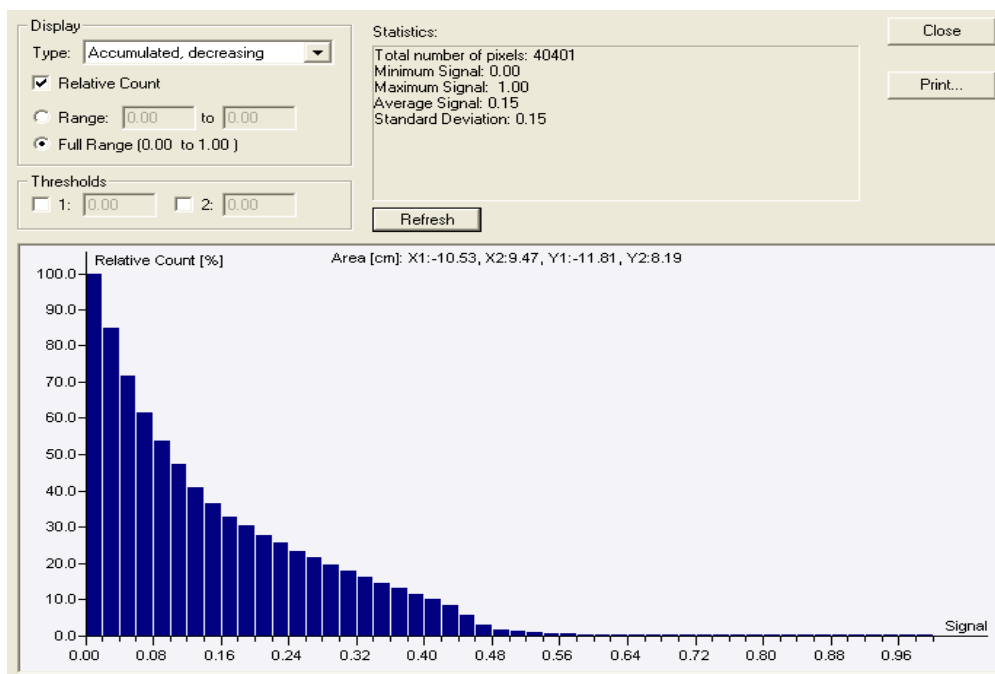
Figure (3.12, b) Gamma index histogram for field 7.

Table (3-12) shows the difference in dose distribution between the measured films and the reconstructed ones from EPID in comparison with the TPS in terms of SD.

Table (3-12) gamma evaluation comparison for the fields as a total between EPID and films.

Field number	EPID SD %	Film SD %	Number of segments
1	0.30	0.33	14
2	0.25	0.26	9
3	0.28	0.27	9
4	0.16	0.31	12
5	0.20	0.32	13
6	0.18	0.30	8
7	0.15	0.28	8
Average	0.21	0.29	

From table (3-12) if the data is analyzed separately either for EPID or for films it will be clear that increasing the number of segments in the plan, increase the value of the SD for both EPID and films that indicate that the deviation is due to the TPS calculation accuracy for either multileaf collimator leaf-end leakage or inter-leaf leakage.

For films and EPID the percentage of pixels passing the gamma test in the region of interest for each field as are shown in figure (3.13.).
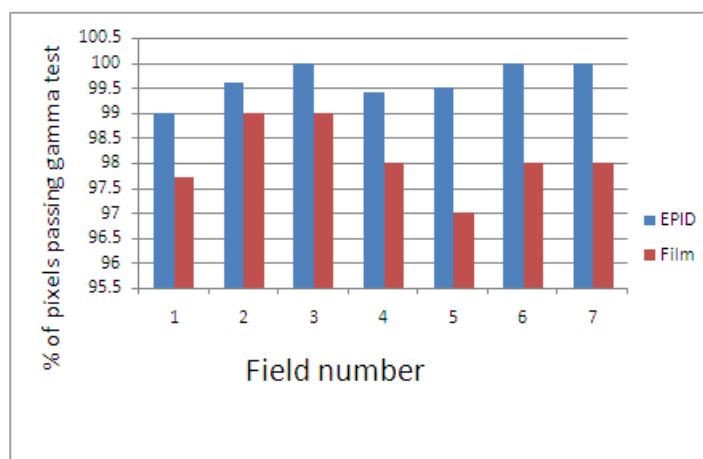
Figure (3.13.) shows the percent of pixel passing the gamma test for EPID against films for each field.

From figure (3.13.) it is clear that all the fields reconstructed from EPID are above 99% (for the criteria 3% dose or 3mm distance to agreement).

Khan,et al, (2008) used 9 beam step-and-shoot IMRT plan for head phantom irradiated with 6MV X-ray and the gamma evaluation histograms calculated for all9 beams indicates that 95% of all points pass the preset criteria 3% dose or 3mm distance to agreement for each field.

IV.   Conclusion

From this study one may conclude the following:

- The time required to perform dose reconstruction with the EPID (iViewGT, release 3.2) is probably the same as the established method using film. Yet, EPID as QA device has advantages over film QA in that it is linear, more reproducible, and eliminates film problems, with scanners.
- The total annual cost of imaging with film is higher than thatusing EPID concerning IMRT QA.
- EPID (iViewGT, release 3.2) can replace the ionization chamber for measuring dose for the studied field sizes at the isocenter at 10cm depth in a 20cm thick PMMA slab phantom at SSD = 90cm after correction for PSF and DF.
- From the study the combination between iViewGTand Omni Pro software with the used corrections can be applied and provides an accurate method to verify the dose of IMRT fields in two dimensions inside a homogenous slab phantom.
- The EPID is an accurate and fast alternative to film for field-by field pretreatment verification of IMRT inside a phantom.

Generally, Michael G. Herman – AAPM Task Group 58 – Electronic Portal Imaging – 2001 shows that the annual cost of imaging with EPID as a function of increasing use of portal imaging is cheaper than that with films. When IMRT QA by films taken into consideration especially that the cost of QA films for IMRT is more expensive than that for portal imaging, sure this cost will be more effective.